

Can Tabular In-Context Learners Generalize to Biomolecular Property Prediction?

Davy Guan^{1,2}, Lu Zhang¹, Asiri Wijesinghe¹, Allen Zhu¹, He Zhao¹, Helen Power¹, F. Hafna Ahmed¹, Andrew Warden¹, Cheng Soon Ong¹, Daniel M. Steinberg¹

¹Commonwealth Scientific and Industrial Research Organisation (CSIRO), Australia

²Computational Pharmacology and Toxicology Laboratory, Sydney Pharmacy School, The University of Sydney

Contact: DGUA4501@UNI.SYDNEY.EDU.AU, DAN.STEINBERG@CSIRO.AU

Abstract

Predicting biomolecular properties from limited labeled data is a central bottleneck in protein engineering and small-molecule design. As strong pretrained encoders now supply rich fixed-length representations, the difficulty has shifted from representation learning to building a data-efficient predictor for the few-shot regime. Tabular foundation models such as TabPFN and TabICL are unlikely candidates for this role: they are in-context learners pretrained on synthetic tables drawn from random causal graphs, a generative prior with no obvious correspondence to the processes that produce protein sequences or molecular graphs. That this tabular, causal inductive bias should transfer to biomolecular data at all is counter-intuitive, yet we find it does. Treating each method as a predictor-representation pair, we evaluate across two domains. We find that on protein fitness regression tasks these in-context learning models coupled with ESM Cambrian representations achieve or exceed state-of-the-art results on ProteinGym, and outperform task-specific supervised regressors on a diverse esterase catalytic activity dataset. For small-molecule classification with ECFP/RDKit descriptors, no single predictor-representation pairing dominates across TDC ADMET, MoleculeNet, FS-Mol, and DrugOOD, but they are competitive with the existing task-specific state-of-the-art. Crucially, on both protein and small-molecule *few-shot* tasks, these predictor-representation pairs offer strong performance. We conclude that tabular foundation models can be strong biomolecular predictors, but only when coupled with expressive representations.

Keywords: tabular foundation models; in-context learning; protein fitness prediction; small-molecule property prediction; few-shot learning

1 Introduction

Predicting the functional consequences of biomolecular data from limited labels is a central problem in protein engineering, variant-effect prediction, and small-molecule design. Deep mutational scanning (DMS) benchmarks such as ProteinGym have greatly improved the scale and rigor of evaluation. In reality however, each new assay typically induces a distinct low-data supervised task in which only a small number of experimentally measured variants are available for a new protein or condition (Notin et al., 2023a; Elnaggar et al., 2022). Recently, large biological foundation models have made sequence representation substantially stronger: protein language models trained on evolutionary corpora provide rich fixed-length embeddings that can be reused across downstream tasks (Elnaggar et al., 2022; Lin et al.,

arXiv:2606.31126v2 [cs.LG] 8 Jul 2026

2023; Hayes et al., 2025). This shifts part of the modeling bottleneck from representation learning to the design of a data-efficient predictor that can exploit those embeddings in the few-shot regime.

Tabular foundation models offer a compelling approach to this bottleneck. Rather than training a new predictor from scratch for each dataset, they amortize Bayesian-style prediction offline over synthetic tabular tasks and perform inference by conditioning on labeled support examples at test time, without task-specific gradient updates (Hollmann et al., 2023, 2025; Qu et al., 2025, 2026). Recent work has extended this paradigm to larger contexts, broader task families, and more realistic data regimes. Science-domain evaluations in metabolomics, analytical chemistry, and materials informatics suggest that these models can transfer effectively once domain-specific structure has been encoded as feature vectors (Wu et al., 2026; Granitto et al., 2026; Li et al., 2026).

It remains an open question whether this transfer holds for two domains with distinct representation challenges and output types: protein fitness regression and small-molecule property classification. Protein fitness prediction requires mapping high-dimensional sequence embeddings to continuous fitness values across hundreds of structurally diverse assays with as few as $\mathcal{O}(10)$ labeled examples. Small-molecule property classification poses a different challenge: representations range from fixed fingerprint vectors to learned molecular graph embeddings, and evaluation must simultaneously capture in-distribution accuracy, low-shot sample efficiency, and out-of-distribution generalization across scaffold, assay, and molecular-size shifts.

We study both settings as an evaluation problem using existing pretrained models and fingerprinting techniques. For protein fitness regression, we encode sequences with ESM-Cambrian (Hayes et al., 2025, referred to as ESMC) and benchmark TabICL (version 2) and TabPFN (version 3) against supervised baselines across ProteinGym and a newly published diverse esterase family dataset (Ahmed et al., 2026). For small-molecule property classification, we evaluate predictor-representation pairs, pairing tabular models with molecular descriptor views and comparing against graph-based baselines. We benchmark across TDC ADMET (Huang et al., 2021), MoleculeNet (Wu et al., 2018), FS-Mol (Stanley et al., 2021), and DrugOOD (Ji et al., 2023), with DrugOOD providing an explicit out-of-domain (OOD) generalization test.

Our contribution is primarily empirical and methodological. We provide a benchmarked audit of tabular foundation models in scientific prediction settings that have not yet been evaluated systematically, and we do so under protocols designed to support cautious, track-appropriate claims. We keep feature pipelines fixed where possible, separate few-shot from full-train conclusions, and treat OOD behavior, official ProteinGym holdouts, benchmark coverage, and support-set sensitivity as first-class parts of the evaluation.

2 Background and Related Work

The prior-data fitted network (PFN) framework trains a transformer offline on synthetic tabular tasks so that prediction can be performed at inference time by conditioning on labelled in-context examples, without task-specific gradient updates (Müller et al., 2022). TabPFN established this formulation for small classification problems and showed that amortized inference over synthetic Bayesian priors can match or exceed carefully tuned

baselines on real benchmarks (Hollmann et al., 2023, 2025). The version 3, 2026 release (Grinsztajn et al., 2026), referred to throughout this paper as TabPFN3, extends the framework with improved scalability and regression support. TabICL scales the paradigm through a two-stage architecture: a first stage applies column-then-row attention to compress each sample into a fixed-dimension row embedding, and a second stage applies a transformer across row embeddings for in-context prediction (Qu et al., 2025, 2026). TabFM is a recent zero-shot tabular foundation model that also treats train and query rows as an in-context prediction problem rather than fitting dataset-specific weights (Google Research, 2026). Because it combines row/column attention, row-level compression, and a transformer over compressed row embeddings, we include TabFM on PpEST as a targeted diagnostic of whether newer tabular ICL architectures alone improve biomolecular transfer. We refer to the TabICL v2 implementation used in this study as TabICL for readability.

For protein prediction tasks, ProteinGym standardizes evaluation across 217 DMS assays spanning diverse proteins and fitness phenotypes, enabling systematic comparison across assay types and substitution depths (Notin et al., 2023a). The dominant supervised strategy pairs a large pretrained sequence encoder with a lightweight task-specific predictor. Protein language models including ProtTrans (Elnaggar et al., 2022), ESM2 (Lin et al., 2023), and ESMC (Hayes et al., 2025) are trained on evolutionary sequence corpora so that their embeddings capture structural and functional constraints learned from natural variation.

Small-molecule property prediction spans ADMET profiling, activity prediction, and out-of-distribution generalization across chemical series. MoleculeNet (Wu et al., 2018), TDC ADMET (Huang et al., 2021), FS-Mol (Stanley et al., 2021), and DrugOOD (Ji et al., 2023) provide complementary regimes covering standard supervised settings, few-shot learning with task-level variation, and systematic distribution shift across scaffolds, assays, and molecular sizes. Fixed descriptors such as ECFP fingerprints (Rogers and Hahn, 2010) and RDKit features expose tabular feature vectors, while graph models such as ChemProp (Yang et al., 2019) and CheMeleon-initialized ChemProp (Burns et al., 2025) model molecular structure directly.

3 Using Tabular ICL Models for Biomolecules

Across both domains we follow a single recipe. A frozen domain encoder maps each biomolecule to a fixed-length feature vector, and that vector becomes one row of an input table for a tabular in-context learner. The predictors, TabICL and TabPFN3, predict the label of a query molecule by conditioning on labeled support rows in context. Protein fitness is treated as regression and reported by MSE and Spearman rank correlation. Small-molecule property prediction is treated as binary classification and reported by ROC-AUC.

Protein representations. Protein sequences are encoded with ESMC (Hayes et al., 2025), a successor to ESM2 (Lin et al., 2023). We use ESMC300M sequence embeddings as the default protein feature set. We additionally test ESMC600M in two roles: mutation-aware features for ProteinGym and sequence-level embeddings for a new diverse esterase dataset, PpEST (Ahmed et al., 2026). The ProteinGym ESMC600M rows augment the mutant mean embedding with wildtype-relative mean deltas, absolute deltas, mutation-site token features, simple mutation descriptors, and zero-shot scores. This distinction matters because ProteinGym assays are single-protein mutation tables, whereas PpEST compares

diverse homologous sequences across assay conditions. For TabICL on the high-dimensional ProteinGym ESMC600M matrix, we use PCA500 because full-dimensional inference exceeded available memory or wall-time limits.

Molecule features. For small molecules, the tabular learners receive either ECFP/Morgan fingerprints (Rogers and Hahn, 2010), RDKit two-dimensional physicochemical descriptors, or their concatenation. The choice of descriptor is an integral part of the model pair since a tabular learner with ECFP features and the same learner with RDKit descriptors can behave very differently. As structural alternatives to fixed descriptors, graph baselines consume molecular graphs directly through ChemProp (Yang et al., 2019) trained from scratch and a foundation-model-initialized variant that fine-tunes ChemProp from the CheMeleon checkpoint (Burns et al., 2025).

4 Protein Prediction Experiments

We evaluate TabICL and TabPFN3 in two protein prediction settings. The first is ProteinGym’s 217 DMS tasks, and the second is the PpEST esterase-family dataset introduced in Ahmed et al. (2026). We test these models in full-training tasks and few-shot settings with 8 to 64 training samples to approximate low-throughput wet-lab measurement regimes.

Datasets. **ProteinGym** (Notin et al., 2023a) is a large-scale collection of DMS assays curated to benchmark computational models of protein fitness. Each assay quantifies the effect of amino acid substitutions on a biologically relevant property. We use the 217 supervised-substitution assays available in the staged evaluation files and report both random 5-fold results and the official random, modulo, and contiguous holdout schemes. **PpEST** is a diverse esterase dataset containing 1513 ancestrally related sequences after excluding approximately 600 sequences partially selected using ML methods. It includes catalytic reaction rates for three ester substrates and thermostability measurements at two temperatures (Ahmed et al., 2026).

Baselines. We compare TabICL and TabPFN3 with ridge regression, RBF sampler, HistGradientBoostingRegressor (HGBR) (Pedregosa et al., 2011), and fine-tuned ESMC with a task-specific MLP regression head. All baselines receive the same ESMC embeddings as inputs.

Evaluation metrics. Protein fitness prediction is evaluated by mean squared error (MSE) and the Spearman rank correlation coefficient. Spearman is the primary ranking metric for comparison with ProteinGym-style variant-effect evaluation, while MSE captures calibrated regression error on the assay scale. For few-shot learning-curve plots, we compute raw MSE and Spearman at each support size and plot a monotone best-so-far envelope over increasing support sizes, k :

$$\text{MSE}_i^+ = \min \{ \text{MSE}_i, \text{MSE}_{i-1}^+ \}, \quad \text{MSE}_1^+ = \text{MSE}_1, \quad (1)$$

$$\text{Spearman}_i^+ = \max \{ \text{Spearman}_i, \text{Spearman}_{i-1}^+ \}, \quad \text{Spearman}_1^+ = \text{Spearman}_1. \quad (2)$$

Here i indexes the few-shot training size, $k \in \{n_1, \dots, n_i, \dots, n_I\}$ and $n_i < n_{i+1}$. This plotting convention avoids visually overemphasizing non-nested support-set noise. The

envelope is used only for visualization; quantitative comparisons use raw support-size summaries.

Experimental settings. In the full-train regime, about 20% of samples are selected for testing. For ProteinGym, we use five-fold cross-validation and report the mean score averaged across assays. For PpEST, we randomly select 20% of samples as the test set. In the few-shot regime, training sizes are 8, 16, 32, and 64. We run 30 repeated support-set draws for each size using stratified quantile-bin sampling to encourage coverage of the observed fitness range.

4.1 ProteinGym Results

Table 1 reports model performance on ProteinGym under the random 5-fold cross-validation protocol used for the main reproduced comparison.

Model	Spearman	MSE
TabPFN3	0.767 ± 0.172	0.351 ± 0.251
TabICL	0.753 ± 0.178	0.376 ± 0.259
HistGradientBoosting	0.700 ± 0.189	0.439 ± 0.259
Ridge	0.663 ± 0.213	0.601 ± 0.457
FT ESM	0.584	0.611
RBF sampler	0.001 ± 0.028	1.142 ± 0.075

Table 1: ProteinGym random 5-fold full-data summary across 217 assays using ESMC300M features. Values are mean ± assay-level standard deviation where per-assay rows are available; FT ESM is retained from the stored aggregate summary. RBF sampler is an untuned random Fourier feature sanity-check baseline rather than an optimized kernel method.

TabPFN3 achieves the strongest aggregate result, with mean Spearman 0.767 and mean MSE 0.351 across 217 assays. TabICL remains close, with mean Spearman 0.753 and mean MSE 0.376. HistGradientBoosting is the strongest classical baseline, followed by Ridge and FT ESM. The RBF sampler is a legitimate but deliberately simple negative-control pipeline: it uses fixed random Fourier features plus ridge regression, and its near-zero Spearman indicates that this untuned kernelization of ESMC space is poorly aligned with assay labels. The two largest assays, HIS7_YEAST_Pokusaeva_2019 and SPG1_STRSG_Olson_2014, required special handling because full-feature inference exceeded practical memory and time limits on the available hardware; the complete rows use PCA rescue settings for those assays.

Table 2 extends the comparison to the official random, modulo, and contiguous ProteinGym fold schemes and adds the ESMC600M representation diagnostic. These values are not directly comparable to Table 1: Table 1 reports our reproduced random 5-fold full-data comparison with ESMC300M features, whereas Table 2 uses the staged ProteinGym official fold columns and includes representation variants. The harder modulo and contiguous splits reduce performance for all configurations, indicating that random-split numbers should not be treated as the only estimate of generalization. ESMC600M improves TabPFN3 overall and across all three schemes, whereas TabICL with the same representation family and PCA500 remains close on the random split but weaker on the harder schemes. The PCA500 suffix is a computational feasibility setting for TabICL on the high-dimensional ESMC600M matrix, not a separate biological representation.

Scheme	Model	Feature set	Spearman	MSE
Overall	TabPFN3	ESMC300M	0.620 ± 0.206	0.583 ± 0.461
Overall	TabPFN3	ESMC600M	0.662 ± 0.195	0.537 ± 0.424
Overall	TabICL	ESMC300M	0.607 ± 0.210	0.603 ± 0.475
Overall	TabICL	ESMC600M-PCA500	0.625 ± 0.202	0.607 ± 0.519
Random	TabPFN3	ESMC300M	0.744 ± 0.177	0.382 ± 0.257
Random	TabPFN3	ESMC600M	0.782 ± 0.163	0.338 ± 0.249
Random	TabICL	ESMC300M	0.729 ± 0.181	0.407 ± 0.266
Random	TabICL	ESMC600M-PCA500	0.773 ± 0.166	0.357 ± 0.283
Modulo	TabPFN3	ESMC300M	0.595 ± 0.177	0.652 ± 0.544
Modulo	TabPFN3	ESMC600M	0.633 ± 0.170	0.610 ± 0.498
Modulo	TabICL	ESMC300M	0.580 ± 0.182	0.669 ± 0.561
Modulo	TabICL	ESMC600M-PCA500	0.584 ± 0.166	0.702 ± 0.622
Contiguous	TabPFN3	ESMC300M	0.522 ± 0.199	0.715 ± 0.464
Contiguous	TabPFN3	ESMC600M	0.570 ± 0.187	0.664 ± 0.410
Contiguous	TabICL	ESMC300M	0.511 ± 0.205	0.732 ± 0.484
Contiguous	TabICL	ESMC600M-PCA500	0.517 ± 0.179	0.762 ± 0.500

Table 2: ProteinGym supervised-substitution performance by official holdout scheme across 217 assays. Values are mean ± assay-level standard deviation; overall rows summarize all assay-scheme cells. ESMC600M denotes the mutation-aware feature set, and TabICL uses PCA500 on that high-dimensional feature matrix. Bold marks the best Spearman per scheme; for MSE, lower is better.

Model	Overall Spearman	Overall MSE
Kermut (Groth et al., 2024)	0.657	0.605
<i>TabPFN3-ESMC600M</i>	0.642	0.591
ProteinNPT (Notin et al., 2023b)	0.619	0.687
<i>TabPFN3-ESMC300M</i>	0.612	0.643
MSA Transformer (Rao et al., 2021)	0.581	0.724

Table 3: Overall ProteinGym supervised-substitution context for the top-ranking entries and the two TabPFN3 configurations. Leaderboard-context rows are sourced from ProteinGym benchmark outputs (ProteinGym, 2026); values use ProteinGym benchmark aggregation, so they need not equal plain assay means. Higher Spearman and lower MSE are better.

Table 3 places the two TabPFN3 configurations in leaderboard context. TabPFN3-ESMC600M improves substantially over TabPFN3-ESMC300M and achieves the lowest overall MSE among these rows, while Kermut remains the strongest overall Spearman reference.

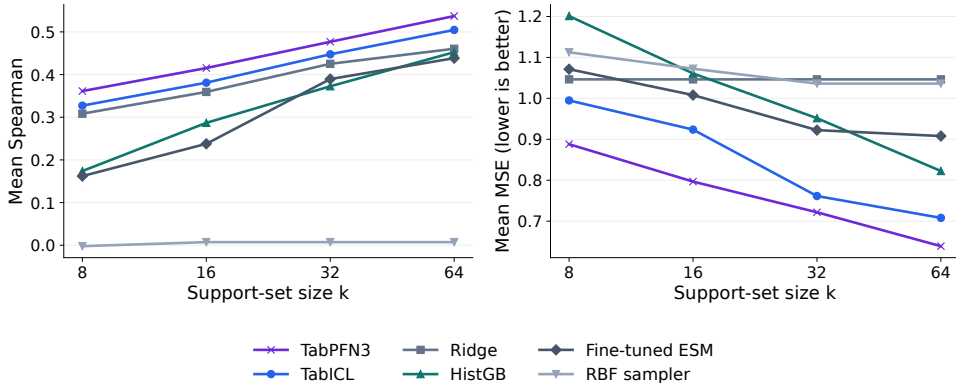


Figure 1: ProteinGym few-shot performance as support-set size increases. Curves show best-so-far task-averaged trends for Spearman and MSE for TabPFN3, TabICL, and supervised baselines. The envelope is used only for visualization; quantitative comparisons use raw support-size summaries.

Model	Spearman k=8	MSE k=8	Spearman k=64	MSE k=64
TabPFN3	0.361 ± 0.247	0.888 ± 0.276	0.537 ± 0.244	0.639 ± 0.262
TabICL	0.327 ± 0.255	0.995 ± 0.387	0.505 ± 0.250	0.708 ± 0.362
Ridge	0.308 ± 0.259	1.046 ± 0.402	0.461 ± 0.257	1.150 ± 1.122
HistGB	0.174 ± 0.195	1.201 ± 0.330	0.452 ± 0.239	0.823 ± 0.498
Fine-tuned ESM	0.162 ± 0.306	1.071 ± 0.187	0.438 ± 0.228	0.908 ± 0.226
RBF sampler	-0.002 ± 0.050	1.113 ± 0.162	-0.003 ± 0.054	1.048 ± 0.166

Table 4: ProteinGym few-shot summary at the smallest and largest support sizes. Values are mean ± standard deviation across assays; MSE is computed on the assay-standardized target scale. The $k = 64$ aggregate contains 216 assays because one assay has only 63 variants.

Figure 1 and Table 4 show best-so-far Spearman and MSE as a function of the number of training samples $k \in \{8, 16, 32, 64\}$. TabPFN3 is strongest at both endpoint support sizes, improving from Spearman 0.361 and MSE 0.888 at $k = 8$ to Spearman 0.537 and MSE 0.639 at $k = 64$. TabICL remains close, with Spearman 0.327 and MSE 0.995 at $k = 8$, and Spearman 0.505 and MSE 0.708 at $k = 64$. The learning curves support the interpretation that tabular in-context models can exploit local structure in ESMC embedding space from very limited labeled examples, while the table records cross-assay variability that is intentionally omitted from the main curves for legibility.

4.2 PpEST Results

Table 5 reports mean full-training results across the five PpEST endpoints, compares ESMC300M with ESMC600M feature sets, retains the original no-PCA TabICL ESMC300M row, and includes TabFM (Google Research, 2026) only as a PpEST diagnostic because it was not competitive enough to carry forward into the ProteinGym experiments.

Model	Feature set	PCA	Spearman	MSE
TabPFN3	ESMC300M	none	0.661 \pm 0.065	0.640 \pm 0.106
TabPFN3	ESMC600M	none	0.658 \pm 0.060	0.631 \pm 0.098
TabICL	ESMC300M	none	0.647 \pm 0.074	0.637 \pm 0.097
TabICL	ESMC300M	500	0.643 \pm 0.074	0.687 \pm 0.107
TabICL	ESMC600M	500	0.625 \pm 0.079	0.678 \pm 0.072
TabFM	ESMC300M	32	0.648 \pm 0.078	0.637 \pm 0.099
TabFM	ESMC600M	32	0.644 \pm 0.072	0.645 \pm 0.097
TabFM	ESMC300M	500	0.642 \pm 0.086	0.639 \pm 0.073
TabFM	ESMC600M	500	0.649 \pm 0.079	0.642 \pm 0.081

Table 5: Full-training performance averaged over the five PpEST endpoints. Values are mean \pm endpoint-level standard deviation. TabFM is included only as a PpEST diagnostic and is not carried forward to ProteinGym because it does not improve over TabPFN3 in this setting. ESMC600M improves MSE for TabPFN3 but does not improve the primary Spearman ranking result over ESMC300M. The no-PCA TabICL row is the original ESMC300M setting.

On PpEST, the representation story differs from ProteinGym. ESMC600M sequence-level features reduce TabPFN3 MSE but do not improve mean Spearman over ESMC300M. For TabICL, PCA is not neutral on this task: the original no-PCA ESMC300M setting is stronger than the PCA500 rows, and ESMC600M-PCA500 does not recover the lost rank correlation. TabFM is close in some PCA settings but does not provide a clean improvement over TabPFN3.

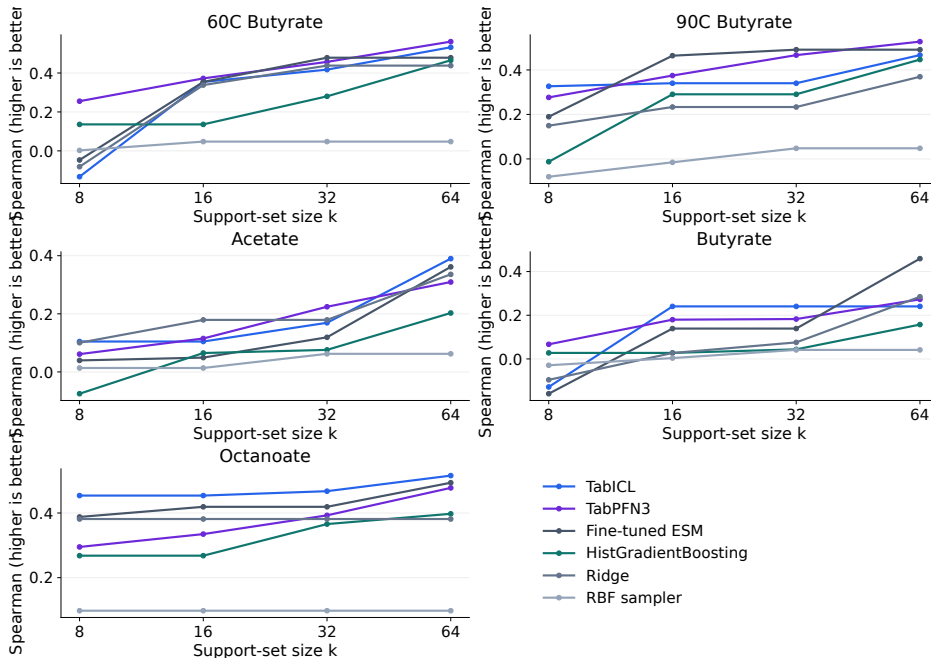


Figure 2: Few-shot PpEST performance measured by Spearman correlation. Curves show monotone best-so-far envelopes over support-set size. The envelope is used only for visualization; quantitative comparisons use raw support-size summaries.

Figure 2 shows that TabICL and TabPFN3 exhibit strong rank preservation in the few-shot regime. Across many PpEST endpoints, one of the two tabular foundation models

achieves the highest or near-highest Spearman correlation, indicating that they effectively preserve the ordering of protein fitness values even when only a small number of labeled examples are available.

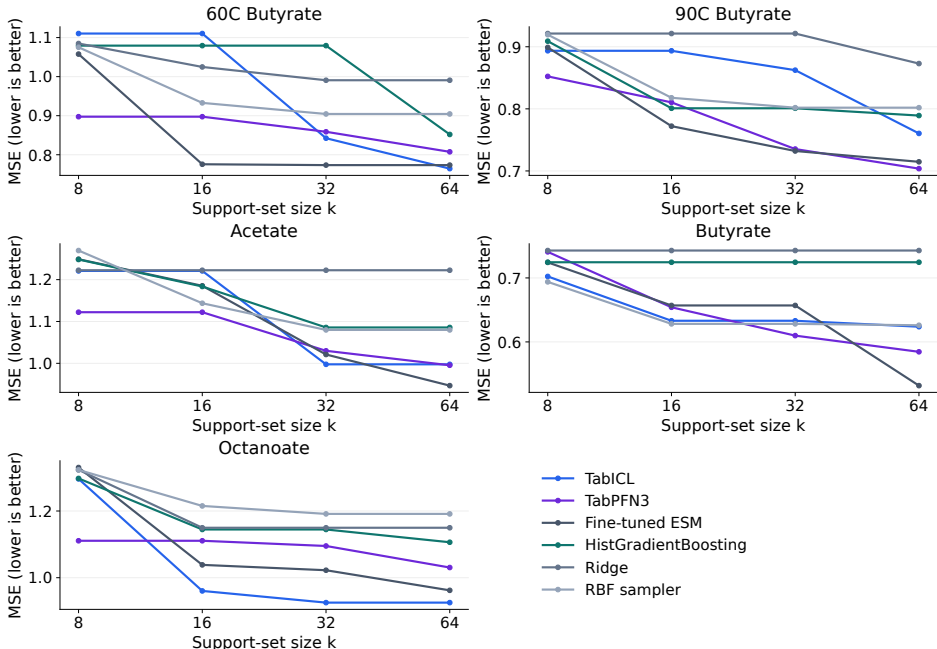


Figure 3: Few-shot PpEST performance measured by MSE. Curves show monotone best-so-far envelopes over support-set size. The envelope is used only for visualization; quantitative comparisons use raw support-size summaries.

Figure 3 shows the corresponding regression-error view. Taken together, PpEST supports a narrower conclusion than ProteinGym: tabular in-context models are effective on ESMC features, but larger sequence embeddings and larger tabular foundation models may not automatically improve rank preservation.

5 Small-Molecule Prediction Experiments

We now evaluate whether the behavior of tabular in-context models transfers from protein sequence embeddings to small-molecule classification. The molecular benchmark covers four public benchmark families: TDC ADMET, MoleculeNet, FS-Mol, and DrugOOD-LBAP-core-IC50. We report predictor-representation pairs rather than pure architectures: TabICL, TabPFN3, and XGBoost use fixed molecular descriptors, whereas ChemProp uses molecular graphs and ChemProp+CheMeleon uses graph foundation-model fine-tuning.

Datasets. **TDC ADMET** (Huang et al., 2021) contains 13 curated small-molecule classification endpoints for absorption, distribution, metabolism, excretion, and toxicity prediction. **MoleculeNet** (Wu et al., 2018) contributes a broad set of molecular classification endpoints, including BBBP, BACE, HIV, ClinTox, SIDER, Tox21, ToxCast, MUV, and PCBA (PubChem BioAssay high-throughput screening endpoints). For multi-label datasets, each label column is treated as a separate binary endpoint. The current classification registry contains 806 MoleculeNet endpoints; full-train TabPFN3 excludes PCBA endpoints

in this report snapshot because those jobs were resource-infeasible under the available rescue attempts. **FS-Mol** (Stanley et al., 2021) contains 157 few-shot molecular property tasks. **DrugOOD-LBAP-core-IC50** (Ji et al., 2023) contains three OOD classification tasks defined by assay, scaffold, and molecular-size shifts.

Benchmark	Role	Tasks/endpoints	Metric
TDC ADMET	ADMET classification	13	Test ROC-AUC
MoleculeNet	Molecular classification	806 registered	Test ROC-AUC
FS-Mol	Few-shot molecular tasks	157	Test ROC-AUC
DrugOOD	OOD classification	3	OOD ROC-AUC

Table 6: Small-molecule benchmark inventory. MoleculeNet full-train TabPFN3 excludes PCBA endpoints in this snapshot after high-memory rescue attempts proved resource-infeasible.

Table 6 summarizes the molecular benchmark inventory. The key distinction from the protein setting is that the molecular experiments combine several benchmark families with different task construction rules and split semantics, so conclusions are reported at the benchmark-family level rather than collapsed into a single global molecular score.

Baselines and metrics. The fixed-feature tabular pairs are TabICL, TabPFN3, and XGBoost (Chen and Guestrin, 2016), each paired with ECFP, RDKit, or ECFP+RDKit features. The graph pairs are ChemProp trained from scratch and ChemProp+CheMeleon. The primary metric is ROC-AUC. For TDC ADMET, MoleculeNet, and FS-Mol, we report benchmark test ROC-AUC. For DrugOOD, the main OOD metric is OOD-test ROC-AUC, and we also report the ID/OOD generalization gap, defined as ID-test ROC-AUC minus OOD-test ROC-AUC. Undefined ROC-AUC values can arise when an evaluation split contains a single class; these rows are treated as undefined split/metric cases rather than model failures. For few-shot learning-curve plots, we use the monotone best-so-far envelope,

$$AUC_i^+ = \max \{AUC_i, AUC_{i-1}^+\}, \quad AUC_1^+ = AUC_1, \quad (3)$$

where i indexes the few-shot training size, $k \in \{n_1, \dots, n_i, \dots, n_I\}$ and $n_i < n_{i+1}$. The envelope is used only for visualization; quantitative comparisons use raw support-size summaries.

Experimental settings. In the few-shot regime, support sets are sampled from the training split only, while validation and test splits remain fixed. We use support sizes $k \in \{8, 16, 32, 64, 128, 256, 512\}$ where feasible and five random seeds by default. In full-train experiments, all available training examples are used where feasible. DrugOOD uses train-once/evaluate-many semantics: each fitted model is evaluated on the ID and OOD test splits without split-specific retraining artifacts.

6 Small-Molecule Results

Figure 4 shows that fixed-feature tabular foundation models remain competitive in low-label molecular prediction, but the ranking depends strongly on both benchmark family and representation. At the largest support size ($k = 512$), TabICL with RDKit descriptors is strongest on MoleculeNet, TabPFN3 with ECFP+RDKit is strongest on FS-Mol, and TabICL RDKit and TabPFN3 ECFP+RDKit are effectively tied on TDC ADMET. On DrugOOD,

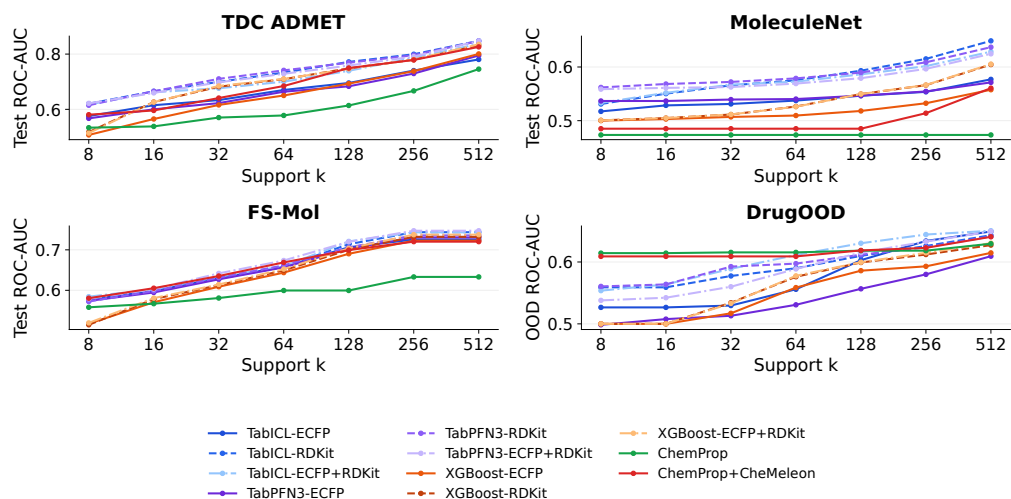


Figure 4: Few-shot small-molecule learning curves. The x-axis is the number of labeled support molecules. The y-axis is test ROC-AUC for TDC ADMET, MoleculeNet, and FS-Mol, and OOD-test ROC-AUC for DrugOOD. Curves show monotone best-so-far envelopes of task-averaged performance across support sizes. The envelope is used only for visualization; quantitative comparisons use raw support-size summaries.

the best few-shot OOD ROC-AUC values are close among TabICL ECFP+RDKit, TabICL ECFP, and TabPFN3 ECFP+RDKit.

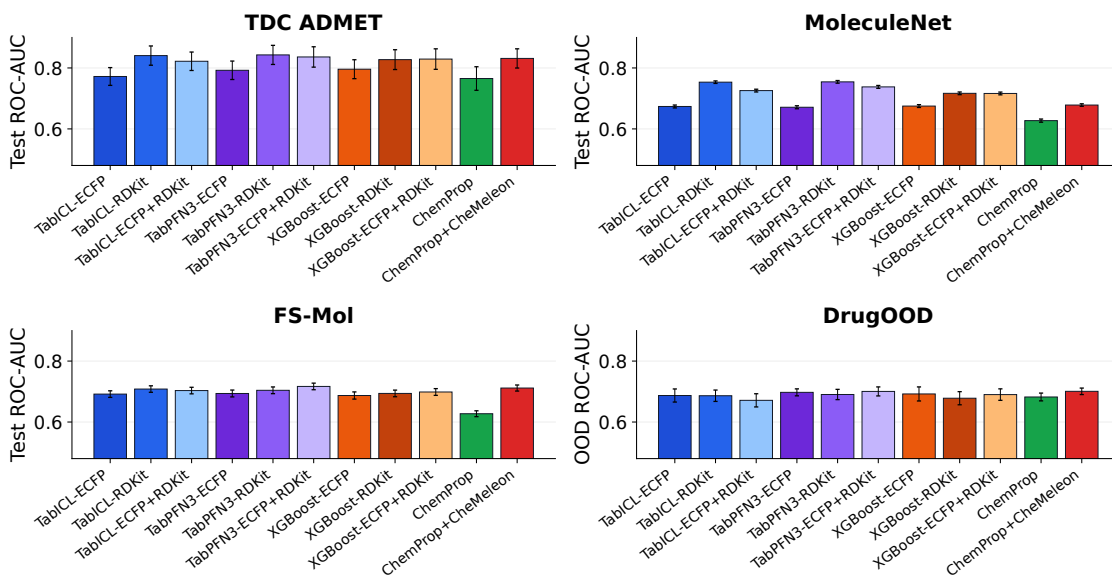


Figure 5: Full-train small-molecule benchmark summary. Bars show mean ROC-AUC across tasks; DrugOOD uses OOD-test ROC-AUC and other benchmark families use benchmark test ROC-AUC.

In the full-train regime, TabPFN3 and TabICL are closely matched on the descriptor-based tasks where both are available. Figure 5 shows that TabPFN3 RDKit slightly exceeds TabICL RDKit on TDC ADMET, while TabPFN3 ECFP+RDKit is strongest on FS-Mol. MoleculeNet full-train TabPFN3 should be interpreted cautiously because PCBA endpoints could not be completed.

Benchmark	Best full-train pair	ROC-AUC	Coverage
TDC ADMET	TabPFN3 RDKit	0.843 \pm 0.113	13/13
MoleculeNet	TabPFN3 RDKit	0.754 \pm 0.113	667/806
FS-Mol	TabPFN3 ECFP+RDKit	0.717 \pm 0.135	157/157
DrugOOD	ChemProp+CheMeleon	0.701 \pm 0.018	3/3

Table 7: Best full-train pair by benchmark family in the current report snapshot. Values are mean \pm task-level standard deviation. MoleculeNet TabPFN3 coverage excludes PCBA endpoints and should not be described as complete MoleculeNet coverage.

Table 7 reinforces the same conclusion: no single predictor-representation pair dominates all molecular benchmark families. TabPFN3 RDKit is strongest on TDC ADMET and the completed non-PCBA MoleculeNet snapshot, TabPFN3 ECFP+RDKit is strongest on FS-Mol, and ChemProp+CheMeleon is strongest on DrugOOD OOD ROC-AUC.

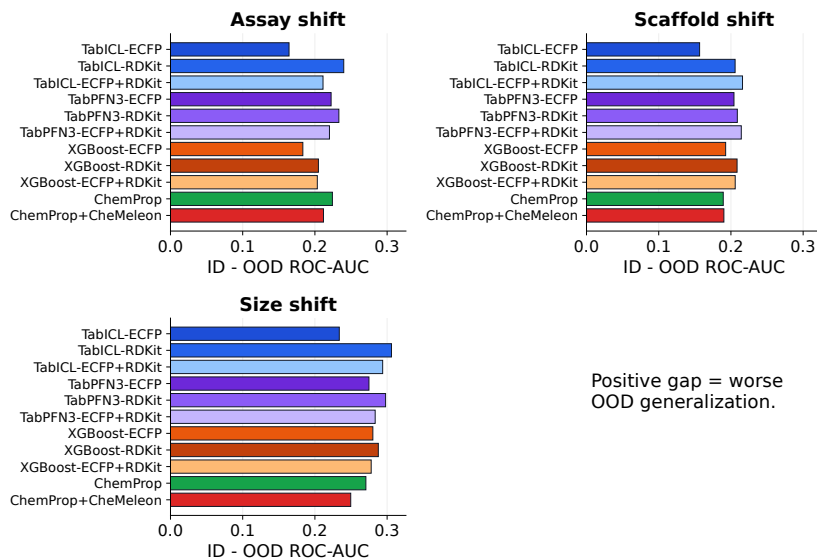


Figure 6: DrugOOD full-train ID/OOD generalization gap. Bars report ID-test ROC-AUC minus OOD-test ROC-AUC for each model pair on assay, scaffold, and molecular-size shifts. Larger positive values indicate a larger performance drop under OOD shift.

DrugOOD shows that in-distribution performance is not sufficient to characterize molecular generalization. Figure 6 shows positive in-domain (ID)/OOD gaps across model families, and the magnitude of the gap depends on both representation and pretraining regime.

The paired TabPFN3-TabICL comparison in Figure 7 gives a more controlled view than aggregate ranking alone. TabPFN3 does not uniformly dominate TabICL: the paired deltas are small overall and change sign by benchmark family and representation. These results support a cautious molecular conclusion: newer tabular foundation models can improve some few-shot settings, but representation choice and task distribution remain first-order determinants of performance.

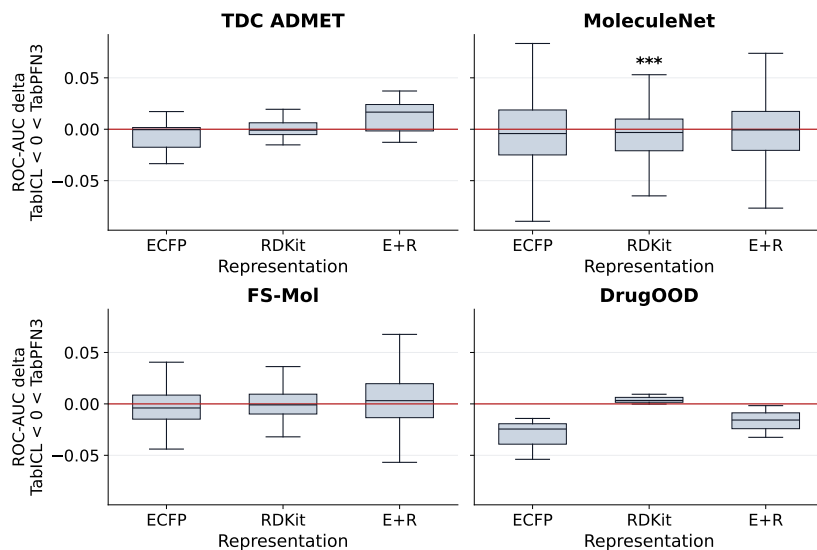


Figure 7: Paired few-shot comparison of TabPFN3 and TabICL on molecules. Positive values favor TabPFN3 and negative values favor TabICL after matching benchmark family, task, molecular representation, support-set size, and seed.

7 Discussion

The main empirical lesson is that tabular foundation models are useful biomolecular predictors, but not as representation-free black boxes. Their behavior is best understood at the level of a predictor-representation pair. A tabular in-context learner can be strong when the frozen representation already exposes task-relevant neighborhood structure, so that nearby rows in feature space tend to have related labels or rankings. This explains why the same learner can look compelling in one biomolecular setting and merely competitive in another: the predictor is not discovering protein biophysics or chemical structure from raw objects, but exploiting the structure made available by ESMC embeddings, molecular fingerprints, RDKit descriptors, or graph features.

The protein results make this dependence especially clear. On ProteinGym, mutation-aware ESMC600M features improve TabPFN3 substantially relative to the earlier ESMC300M configuration, including the lowest aggregate MSE among the leaderboard-context rows considered here. This is a favorable setting for in-context tabular prediction: each assay is a mutation table around a protein background, and the feature representation is explicitly tied to variant effects. The harder modulo and contiguous ProteinGym splits remain much less forgiving than random folds, however, which shows that random-split performance should not be treated as a complete estimate of variant-effect generalization.

PpEST provides a useful counterpoint rather than a contradiction. There, ESMC600M sequence-level features improve TabPFN3 MSE slightly but do not improve the primary Spearman result over ESMC300M. TabICL also shows that PCA compression is not neutral: the original no-PCA ESMC300M row is stronger in rank correlation than the PCA500 variants. This suggests that larger encoders and larger feature matrices are not automatically better for diverse homologous-sequence regression. The representation must match the biological comparison being made: mutation-aware features appear to help in single-protein DMS

tables, whereas sequence-level embeddings for a family-level enzyme dataset can change calibration without preserving rank order.

The molecular experiments show the same principle in a different domain. TabICL and TabPFN3 are competitive with XGBoost and graph baselines in several few-shot and full-train settings, but no learner dominates across TDC ADMET, MoleculeNet, FS-Mol, and DrugOOD. Descriptor choice changes the ranking within the same model family, and graph-based ChemProp+CheMeleon remains strongest in the DrugOOD full-train summary. This supports a cautious practical recommendation: for small-molecule prediction, tabular foundation models should be benchmarked as descriptor-conditioned predictors, not as replacements for molecular representation design.

The TabFM diagnostic strengthens this interpretation. TabFM is a newer tabular foundation model, yet in the PpEST experiments it does not provide a clean improvement over TabPFN3 under the tested ESMC feature settings. This negative result is useful because it rules out a simplistic “newer tabular foundation model is better” story. The decisive factor is not just model scale or recency, but whether the model, representation, and split regime form a compatible prediction problem.

Overall, these results support a more modest but more durable claim than a leaderboard-style model ranking. Tabular in-context learning can be a practical interface between pretrained biological or chemical representations and low-label supervised prediction. Its value is strongest when the representation already organizes examples in a way that makes local interpolation meaningful, and weakest when the feature view, task structure, or distribution shift breaks that assumption. Future benchmarks for in-context learning should therefore report support-set sensitivity, representation choice, and split regime alongside aggregate performance.

Limitations. Several limitations should remain explicit. First, the ESMC600M feature update is not a single interchangeable representation across all protein tasks: ProteinGym uses mutation-aware features that augment mutant embeddings with wildtype-relative and zero-shot descriptors, whereas PpEST uses sequence-level embeddings. Second, TabICL uses PCA500 on ESMC600M because full-dimensional inference was resource-infeasible for large ProteinGym assays. Third, the hardest ProteinGym modulo and contiguous holdout schemes reduce performance for both tabular in-context learners, so random-split numbers should not be interpreted as the only estimate of generalization. Fourth, MoleculeNet full-train TabPFN3 excludes PCBA endpoints because those jobs were resource-infeasible under available rescue attempts. Fifth, molecular ROC-AUC can be undefined for single-class evaluation splits, especially in highly imbalanced endpoints; these rows should be treated as split/metric limitations rather than model failures.

8 Future Directions

The most immediate next step is to turn the predictor-representation framing into a diagnostic tool. Rather than asking only which model wins after a full benchmark run, future work should estimate whether a new assay is likely to benefit from TabPFN3, TabICL, a graph model, or a simpler supervised baseline. Useful predictors may include label smoothness in representation, nearest-neighbor predictability, support-set coverage, assay size, feature dimensionality, and the gap between random and structured holdout splits.

A second direction is support-set, representation, and systems design. Active support selection, diversity-aware support construction, and representation-specific diagnostics could make in-context prediction more useful for prospective wet-lab design. For proteins, mutation-aware, sequence-level, structural, and MSA-derived features should be compared under matched supervised protocols. Large DMS assays and PCBA-like molecular screens also expose scalability limits; future systems should support streaming or sharded inference, predictable memory use, and auditable records of feature construction, split IDs, support-set IDs, rescue settings, and complete predictions.

9 Conclusion

In this work we have answered the question the title poses: tabular foundation models are viable predictors for biomolecular property prediction, but they should not be evaluated as representation-free black boxes. Their strongest use is as part of a predictor-representation pair: ESMC plus TabPFN3 or TabICL for protein regression, and descriptor-specific TabPFN3 or TabICL pairings for molecular classification. They also provide reliable predictive performance in *few-shot* regimes when paired with powerful representations. We believe this is an important takeaway from this work, as many real-world applications only have access to a small number of experimentally measured molecules.

References

- F. Hafna Ahmed, Asher Bender, Asiri Wijesinghe, Allen Zhu, Lu Zhang, Leigh Gebbie, Adrian Marsh, Chie Ishitate, William Holdsworth, Candice Jones, Andrew C. Warden, Helen Power, Cheng Soon Ong, Daniel Steinberg, and Robert E. Speight. Data-efficient exploration of enzyme function using family-specific machine learning. *bioRxiv*, 2026. doi: 10.64898/2026.06.02.729712.
- Jackson Burns, Akshat Zalte, and William H. Green. Descriptor-based foundation models for molecular property prediction, 2025. Preprint, arXiv:2506.15792.
- Tianqi Chen and Carlos Guestrin. Xgboost: A scalable tree boosting system. In *Proceedings of the 22nd ACM SIGKDD International Conference on Knowledge Discovery and Data Mining, KDD '16*, page 785–794, New York, NY, USA, 2016. Association for Computing Machinery. ISBN 9781450342322. doi: 10.1145/2939672.2939785.
- Ahmed Elnaggar, Michael Heinzinger, Christian Dallago, Ghalia Rehawi, Yu Wang, Llion Jones, Tom Gibbs, Tamas Feher, Christoph Angerer, Martin Steinegger, Debsindhu Bhowmik, and Burkhard Rost. Prottrans: Toward understanding the language of life through self-supervised learning. *IEEE Transactions on Pattern Analysis and Machine Intelligence*, 44(10):7112–7127, 2022. doi: 10.1109/TPAMI.2021.3095381.
- Google Research. TabFM: A zero-shot foundation model for tabular data. <https://research.google/blog/introducing-tabfm-a-zero-shot-foundation-model-for-tabular-data/>, 2026.
- Pablo M. Granitto, Emanuela Betta, Iuliia Khomenko, Michele Pedrotti, Andrea Romano, Franco Biasioli, et al. On the use of TabPFN on mass spectrometry analysis of volatile organic compounds. *Scientific Reports*, 16:164, 2026. doi: 10.1038/s41598-025-29128-6.
- Léo Grinsztajn, Klemens Flöge, Oscar Key, Felix Birkel, Philipp Jund, Brendan Roof, Mihir Manium, Shi Bin Hoo, Magnus Bühler, Anurag Garg, Dominik Safaric, Jake Robertson, Benjamin Jäger,

- Simone Alessi, Adrian Hayler, Vladyslav Moroshan, Lennart Purucker, Philipp Singer, Alan Arazi, Julien Siems, Jan Hendrik Metzen, Georg Grab, Nick Erickson, Siyuan Guo, Elliott Kalfon, Simon Bing, David Salinas, Clara Cornu, Lilly Charlotte Wehrhahn, Diana Kriuchkova, Kursat Kaya, Lydia Sidhoun, Marie Salmon, Jerry Chen, Madelon Hulsebos, Yann LeCun, Samuel Müller, Bernhard Schölkopf, Sauraj Gambhir, Noah Hollmann, and Frank Hutter. TabPFN-3: Technical report, 2026.
- Peter Mørch Groth, Mads Herbert Kern, Lars Olsen, Jesper Salomon, and Wouter Boomsma. Kermut: Composite kernel regression for protein variant effects. In *Advances in Neural Information Processing Systems*, volume 37, pages 29514–29565, 2024.
- Thomas Hayes, Roshan Rao, Halil Akin, Nicholas J Sofroniew, Deniz Oktay, Zeming Lin, Robert Verkuil, Vincent Q Tran, Jonathan Deaton, Marius Wiggert, et al. Simulating 500 million years of evolution with a language model. *Science*, 387(6736):850–858, 2025.
- Noah Hollmann, Samuel Müller, Katharina Eggenberger, and Frank Hutter. TabPFN: A transformer that solves small tabular classification problems in a second. In *International Conference on Learning Representations*, 2023.
- Noah Hollmann, Samuel Müller, Lennart Purucker, Arjun Krishnakumar, Max Körfer, Shi Bin Hoo, Robin Tibor Schirrmeyer, and Frank Hutter. Accurate predictions on small data with a tabular foundation model. *Nature*, 637(8045):319–326, 2025. doi: 10.1038/s41586-024-08328-6.
- Kexin Huang, Tianfan Fu, Wenhao Gao, Yue Zhao, Yusuf Roohani, Jure Leskovec, Connor W. Coley, Cao Xiao, Jimeng Sun, and Marinka Zitnik. Therapeutics data commons: Machine learning datasets and tasks for drug discovery and development. In *Proceedings of the Neural Information Processing Systems Track on Datasets and Benchmarks*, volume 1, 2021.
- Yuanfeng Ji, Lu Zhang, Jiayang Wu, Bingzhe Wu, Lanqing Li, Long-Kai Huang, Tingyang Xu, Yu Rong, Jie Ren, Ding Xue, Houtim Lai, Shaoyong Xu, Jing Feng, Wei Liu, Ping Luo, Shuigeng Zhou, Junzhou Huang, Peilin Zhao, and Yatao Bian. DrugOOD: Out-of-distribution (ood) dataset curator and benchmark for ai-aided drug discovery. In *Proceedings of the AAAI Conference on Artificial Intelligence*, volume 37, pages 8023–8031, 2023. doi: 10.1609/aaai.v37i7.26103.
- Qinyang Li, Rongzhi Dong, Nicholas Miklaucic, Jeffrey Hu, Sadman Sadeed Omeed, Lai Wei, Sourin Dey, Ming Hu, and Jianjun Hu. In context learning foundation models for materials property prediction with small datasets. *npj Computational Materials*, 2026. doi: 10.1038/s41524-026-02089-8.
- Zeming Lin, Halil Akin, Roshan Rao, Brian Hie, Zhongkai Zhu, Wenting Lu, Nikita Smetanin, Robert Verkuil, Ori Kabeli, Yaniv Shmueli, Allan dos Santos Costa, Maryam Fazel-Zarandi, Tom Sercu, Salvatore Candido, and Alexander Rives. Evolutionary-scale prediction of atomic-level protein structure with a language model. *Science*, 379(6637):1123–1130, 2023. doi: 10.1126/science.ade2574.
- Samuel Müller, Noah Hollmann, Sebastian Pineda Arango, Josif Grabocka, and Frank Hutter. Transformers can do bayesian inference. In *International Conference on Learning Representations*, 2022.
- Pascal Notin, Aaron Kollasch, Daniel Ritter, Lood Van Niekerk, Steffanie Paul, Han Spinner, Nathan Rollins, Ada Shaw, Rose Orenbuch, Ruben Weitzman, et al. Proteingym: Large-scale benchmarks for protein fitness prediction and design. *Advances in Neural Information Processing Systems*, 36: 64331–64379, 2023a.
- Pascal Notin, Ruben Weitzman, Debora Marks, and Yarin Gal. ProteinNPT: Improving protein property prediction and design with non-parametric transformers. In *Advances in Neural Information Processing Systems*, volume 36, pages 33529–33563, 2023b.

- F. Pedregosa, G. Varoquaux, A. Gramfort, V. Michel, B. Thirion, O. Grisel, M. Blondel, P. Prettenhofer, R. Weiss, V. Dubourg, J. Vanderplas, A. Passos, D. Cournapeau, M. Brucher, M. Perrot, and E. Duchesnay. Scikit-learn: Machine learning in Python. *Journal of Machine Learning Research*, 12:2825–2830, 2011.
- ProteinGym. ProteinGym benchmarks. <https://proteingym.org/benchmarks>, 2026. Accessed July 2026.
- Jingang Qu, David Holzmüller, Gaël Varoquaux, and Marine Le Morvan. TabICL: A tabular foundation model for in-context learning on large data. In *Proceedings of the 42nd International Conference on Machine Learning*, volume 267 of *Proceedings of Machine Learning Research*, pages 50817–50847, 2025.
- Jingang Qu, David Holzmüller, Gaël Varoquaux, and Marine Le Morvan. Tabiclv2: A better, faster, scalable, and open tabular foundation model, 2026. Preprint, arXiv:2602.11139.
- Roshan M. Rao, Jason Liu, Robert Verkuil, Joshua Meier, John Canny, Pieter Abbeel, Tom Sercu, and Alexander Rives. MSA transformer. In *Proceedings of the 38th International Conference on Machine Learning*, volume 139 of *Proceedings of Machine Learning Research*, pages 8844–8856. PMLR, 2021. URL <https://proceedings.mlr.press/v139/rao21a.html>.
- David Rogers and Mathew Hahn. Extended-connectivity fingerprints. *Journal of Chemical Information and Modeling*, 50(5):742–754, 2010. doi: 10.1021/ci100050t.
- Megan Stanley, John F. Bronskill, Krzysztof Maziarz, Hubert Misztela, Jessica Lanini, Marwin Segler, Nadine Schneider, and Marc Brockschmidt. FS-Mol: A few-shot learning dataset of molecules. In *Proceedings of the Neural Information Processing Systems Track on Datasets and Benchmarks*, volume 1, 2021.
- Dan-Ni Wu, Joey Jen, Erickson Fajiculay, Min-Fen Hsu, Ming-Chu Chang, Jen-Chen Yeh, Karen Sargsyan, Juozas Kupcinskas, Jurgita Skieceviciene, Ruta Steponaitiene, Egidijus Morkunas, Greta Gedgaudiene, Chao-Ping Hsu, Yu-Ting Chang, Chun-Mei Hu, et al. PanMETAI - a high performance tabular foundation model for accurate pancreatic cancer diagnosis via NMR metabolomics. *Nature Communications*, 17:1595, 2026. doi: 10.1038/s41467-026-69426-9.
- Zhenqin Wu, Bharath Ramsundar, Evan N. Feinberg, Joseph Gomes, Caleb Geniesse, Aneesh S. Pappu, Karl Leswing, and Vijay Pande. MoleculeNet: A benchmark for molecular machine learning. *Chemical Science*, 9(2):513–530, 2018. doi: 10.1039/C7SC02664A.
- Kevin Yang, Kyle Swanson, Wengong Jin, Connor Coley, Philipp Eiden, Hua Gao, Angel Guzman-Perez, Timothy Hopper, Brian Kelley, Miriam Mathea, Andrew Palmer, Volker Settels, Tommi Jaakkola, Klavs Jensen, and Regina Barzilay. Analyzing learned molecular representations for property prediction. *Journal of Chemical Information and Modeling*, 59(8):3370–3388, 2019. doi: 10.1021/acs.jcim.9b00237.